

Numerical Diffusion and Dispersion Tensors for 2-D Linear Advection Equation

Małgorzata Bielecka-Kieloch

Institute of Hydro-Engineering of the Polish Academy of Sciences, ul. Kościarska 7,
80-953 Gdańsk, Poland

(Received July 15, 1998; revised December 29, 1998)

Abstract

An improvement of the methodology used in the evaluation of numerical errors occurring in solution of the 2-D advection equation is proposed in the paper. For this reason numerical diffusion and dispersion tensors are introduced. Using an example of the upwind scheme the methodology for derivation of numerical diffusion and dispersion tensors is presented and analysis abilities that they provide are discussed. Numerical and physical diffusion coefficients are compared for a chosen example.

1. Introduction

The 2-D advection-diffusion equation is commonly used for solving various problems concerning such physical phenomena as: mass, energy and momentum transport. Since in most cases an analytical solution is not possible, numerical methods are applied. Unfortunately, these methods are responsible for serious numerical problems which result both from numerical methods limitations and requirements, as well as from the sole nature of the advection-diffusion equation. As we know, approximation of the advective term existing in this equation is the reason for most numerical problems. Discretization of the equation introduces numerical diffusion and dispersion to the solution. Due to numerical diffusion an inaccurate solutions is obtained. On the other hand numerical dispersion is responsible for oscillations in the solution. Such errors are the result of truncation of second and third order terms of Taylor series expansion, which is used in determination of finite differences, approximating derivatives occurring in the advection-diffusion equation. These terms decide as to the accuracy of a solution. In this situation it is very important to have the ability to determine the magnitude of the errors generated. In the case of a 1-D linear equation they have a relatively clear and simple form, so their interpretation is not troublesome. Unfortunately in the 2-D case the form of the error resulting from the Taylor series truncation becomes much more complicated, since there appear terms including derivatives in the second

direction as well as mixed derivatives. Analysis of the errors may be simplified by the introduction of so-called numerical diffusion and dispersion tensors. The proposal to introduce tensors seems to be attractive. As the review of literature shows, this kind of approach has not been presented up till now. For instance Fletcher (Fletcher 1991) determines artificial diffusivity for a 2-dimensional case, but only for normal and longitudinal directions to the flow, since from the physical point of view their meaning is most significant. Apart from this the analysis is performed for an advection-diffusion equation steady in time and restricted to numerical diffusion only.

B. J. Noye and H. H. Tan (Noye and Tan 1989) have also conducted accuracy analyses of some differential schemes used in solving 2-dimensional advection-diffusion equations. The analyses concerned various schemes with finite differences but no generalization has been introduced to either the methods themselves or derived formulas describing numerical diffusion. The numerical dispersion has not been analyzed at all.

In this paper a method for the derivation of numerical diffusion and dispersion tensors for the solution of a 2-D linear advection equation is proposed and analysis possibilities that they provide are discussed. This can be presented on the example of the well-known upwind scheme.

2. Formulation of the Problem

Let us assume that transport of a conservative substance dissolved in water in a two-dimensional case, without source terms, is described by the following linear differential equation, depicted in the Cartesian co-ordinate system:

$$\frac{\partial f}{\partial t} + u_j \frac{\partial f}{\partial x_j} - \frac{\partial}{\partial x_j} \left(\mathbf{K}^d \frac{\partial f}{\partial x_j} \right) = 0, \quad (1)$$

where:

$$j = 1, 2$$

$$u_1 = u, u_2 = v,$$

$$u, v$$

– velocity vector components in x and y directions respectively,

$$x_1 = x, x_2 = y$$

– space coordinates,

$$\mathbf{K}^d$$

– diffusivity tensor defined as follows:

$$\mathbf{K}^d = \begin{bmatrix} K_{xx} & K_{xy} \\ K_{yx} & K_{yy} \end{bmatrix} \quad (1a)$$

For Eq. (1) the initial-boundary problem is formulated where a solution (usually numerical) represents a function $f(x, y, t)$ for $x, y \in S$ (where S is the solution domain) and $t \geq 0$. The function $f(x, y, t)$ has to be continuous and differentiable.

When the diffusive term is neglected, Eq. (1) becomes a pure advection equation:

$$\frac{\partial f}{\partial t} + u \frac{\partial f}{\partial x} + v \frac{\partial f}{\partial y} = 0. \tag{2}$$

Let us solve this equation by applying a rectangular grid of dimensions $\Delta x \cdot \Delta y$ (Fig. 1) and assuming for simplification $u, v = \text{const}$.

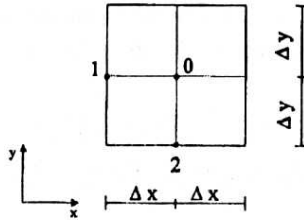


Fig. 1. Differential grid for an upwind scheme

Approximation of derivatives in node "0" at time level $t + \theta \Delta t$ with use of the upwind scheme, results in the following differential equation:

$$\begin{aligned} \frac{f_0^{k+1} - f_0^k}{\Delta t} + \theta \left(u \frac{f_0^{k+1} - f_1^{k+1}}{\Delta x} + v \frac{f_0^{k+1} - f_2^{k+1}}{\Delta y} \right) + \\ - (1 - \theta) \left(u \frac{f_0^k - f_1^k}{\Delta x} + v \frac{f_0^k - f_2^k}{\Delta y} \right) = 0, \end{aligned} \tag{3}$$

where:

- k - index of time level,
- Δt - time step,
- θ - weighting parameter from the range $\langle 0, 1 \rangle$.

The value of the function f at time level $k + 1$ in question equals:

$$\begin{aligned} f_0^{k+1} = f_0^k - \theta \left[C_x (f_0^{k+1} - f_1^{k+1}) + C_y (f_0^{k+1} - f_2^{k+1}) \right] + \\ - (1 - \theta) \left[C_x (f_0^k - f_1^k) + C_y (f_0^k - f_2^k) \right], \end{aligned} \tag{4}$$

where:

$$C_x = u \Delta t / \Delta x, \quad C_y = v \Delta t / \Delta y \tag{5}$$

are the advective Courant numbers in x and y directions respectively. Properties of this scheme depend on the parameter θ , which can be proved by stability and accuracy analysis.

The numerical stability analysis has been performed applying the Neumann method (Fletcher 1991). It has been proved that the stability condition is satisfied when (Bielecka-Kieloch 1998):

$$(C_x + C_y)(1 - 2\theta) - 1 \leq 0 \quad (6)$$

It should be noticed that for

$$\theta \geq 1/2 \quad (7)$$

the foregoing relation is always true for all Courant numbers C_x and C_y , and the scheme is absolutely stable. However, for $\theta < 1/2$ the scheme is stable if

$$C_x + C_y \leq \frac{1}{(1 - 2\theta)}. \quad (8)$$

If $\theta = 0$ is assumed, the stability condition for the classical explicit upwind scheme is obtained.

3. Accuracy Analysis

In the Eq. (3) the nodal values are replaced by their estimates resulting from Taylor-series expansion of the function f in node 0 at time level $t + \theta \Delta t$. In the series terms with up to third-order derivatives are included. As a result of transformation the following expression is obtained (Bielecka-Kieloch, 1998):

$$\begin{aligned} & \frac{\partial f_0}{\partial t} + \left(\frac{1}{2} - \theta\right) \Delta t \frac{\partial^2 f_0}{\partial t^2} + (1 - 3\theta + 3\theta^2) \frac{\Delta t^2}{6} \frac{\partial^3 f_0}{\partial t^3} + \theta \left[u \frac{\partial f_0}{\partial x} + v \frac{\partial f_0}{\partial y} + \right. \\ & + \left(-\frac{u \Delta x}{2} \frac{\partial^2 f_0}{\partial x^2} + \frac{u \Delta x^2}{6} \frac{\partial^3 f_0}{\partial x^3} + u(1 - \theta) \Delta t \frac{\partial^2 f_0}{\partial x \partial t} + \right. \\ & \quad \left. - \frac{u(1 - \theta) \Delta t \Delta x}{2} \frac{\partial^3 f_0}{\partial x^2 \partial t} + \frac{u(1 - \theta)^2 \Delta t^2}{2} \frac{\partial^3 f_0}{\partial x \partial t^2} \right) + \\ & + \left(-\frac{v \Delta y}{2} \frac{\partial^2 f_0}{\partial y^2} + \frac{v \Delta y^2}{6} \frac{\partial^3 f_0}{\partial y^3} + v(1 - \theta) \Delta t \frac{\partial^2 f_0}{\partial y \partial t} + \right. \\ & \quad \left. - \frac{v(1 - \theta) \Delta t \Delta y}{2} \frac{\partial^3 f_0}{\partial y^2 \partial t} + \frac{v(1 - \theta)^2 \Delta t^2}{2} \frac{\partial^3 f_0}{\partial y \partial t^2} \right) \left. \right] + (1 - \theta) \left[u \frac{\partial f_0}{\partial x} + v \frac{\partial f_0}{\partial y} + \right. \\ & + \left(-\frac{u \Delta x}{2} \frac{\partial^2 f_0}{\partial x^2} + \frac{u \Delta x^2}{6} \frac{\partial^3 f_0}{\partial x^3} - u \theta \Delta t \frac{\partial^2 f_0}{\partial x \partial t} + \right. \\ & \quad \left. + \frac{u \theta \Delta t \Delta x}{2} \frac{\partial^3 f_0}{\partial x^2 \partial t} + \frac{u \theta^2 \Delta t^2}{2} \frac{\partial^3 f_0}{\partial x \partial t^2} \right) + \\ & + \left(-\frac{v \Delta y}{2} \frac{\partial^2 f_0}{\partial y^2} + \frac{v \Delta y^2}{6} \frac{\partial^3 f_0}{\partial y^3} - v \theta \Delta t \frac{\partial^2 f_0}{\partial y \partial t} + \right. \\ & \quad \left. + \frac{v \theta \Delta t \Delta y}{2} \frac{\partial^3 f_0}{\partial y^2 \partial t} + \frac{v \theta^2 \Delta t^2}{2} \frac{\partial^3 f_0}{\partial y \partial t^2} \right) \left. \right] = 0. \quad (9) \end{aligned}$$

Applying the following relations resulting from (2):

$$\frac{\partial f}{\partial t} = -u \frac{\partial f}{\partial x} - v \frac{\partial f}{\partial y}, \tag{10}$$

$$\frac{\partial^2 f}{\partial t^2} = u^2 \frac{\partial^2 f}{\partial x^2} + v^2 \frac{\partial^2 f}{\partial y^2} + 2uv \frac{\partial^2 f}{\partial x \partial y}, \tag{11}$$

$$\frac{\partial^3 f}{\partial t^3} = -u^3 \frac{\partial^3 f}{\partial x^3} - v^3 \frac{\partial^3 f}{\partial y^3} - 3u^2v \frac{\partial^3 f}{\partial x^2 \partial y} - 3uv^2 \frac{\partial^3 f}{\partial x \partial y^2}, \tag{12}$$

it is possible to transform Eq. (9) in such way that on its left side the advection equation is obtained and on its right side, additional terms resulting from the applied approximation, appear. This equation then takes the following form:

$$\begin{aligned} \frac{\partial f}{\partial t} + u \frac{\partial f}{\partial x} + v \frac{\partial f}{\partial y} = & \left[\left(\theta - \frac{1}{2} \right) \Delta t u^2 + \frac{u \Delta x}{2} \right] \frac{\partial^2 f}{\partial x^2} + \\ & + \left[\left(\theta - \frac{1}{2} \right) \Delta t v^2 + \frac{v \Delta y}{2} \right] \frac{\partial^2 f}{\partial y^2} + 2 \left(\theta - \frac{1}{2} \right) \Delta t uv \frac{\partial^2 f}{\partial x \partial y} + \\ & + u \Delta x^2 \left[\left(1 - 6\theta + 6\theta^2 \right) \frac{C_x^2}{6} - \frac{\Delta x}{6} \right] \frac{\partial^3 f}{\partial x^3} + \\ & + v \Delta y^2 \left[\left(1 - 6\theta + 6\theta^2 \right) \frac{C_y^2}{6} - \frac{\Delta y}{6} \right] \frac{\partial^3 f}{\partial y^3} + \\ & + v \Delta x^2 (1 - 6\theta + 6\theta^2) \frac{C_x^2}{2} \frac{\partial^3 f}{\partial x^2 \partial y} + u \Delta y^2 (1 - 6\theta + 6\theta^2) \frac{C_y^2}{2} \frac{\partial^3 f}{\partial x \partial y^2}. \end{aligned} \tag{13}$$

The second order terms on the right side are responsible for numerical diffusion and the third order terms - for numerical dispersion. If they are expressed in the form of a tensor then an equation analogical to Eq. (1) is obtained, with the difference that the right side describes not physical, but numerical effects. According to this analogy Eq. (13) can be written as follows (Bielecka-Kieloch, 1998):

$$\frac{\partial f}{\partial t} + u_i \frac{\partial f}{\partial x_i} = \frac{\partial}{\partial x_i} \left(\mathbf{D}^n \frac{\partial f}{\partial x_j} \right) - \frac{\partial}{\partial x_i} \left(\mathbf{T}^n \frac{\partial^2 f}{\partial x_n^2} \right) + \dots, \tag{14}$$

where:

$$\mathbf{D}^n = \begin{bmatrix} \left(\theta - \frac{1}{2} \right) \Delta t u^2 + \frac{u \Delta x}{2} & \left(\theta - \frac{1}{2} \right) \Delta t uv \\ \left(\theta - \frac{1}{2} \right) \Delta t vu & \left(\theta - \frac{1}{2} \right) \Delta t v^2 + \frac{v \Delta y}{2} \end{bmatrix} \tag{15a}$$

$$\mathbf{T}^n = \begin{bmatrix} u\Delta x^2 \left[\frac{1}{6} - r \frac{C_x^2}{6} \right] & -u\Delta y^2 r \frac{C_y^2}{2} \\ -v\Delta x^2 r \frac{C_x^2}{2} & v\Delta y^2 \left[\frac{1}{6} - r \frac{C_y^2}{6} \right] \end{bmatrix} \quad (15b)$$

$$r = 1 - 6\theta + 6\theta^2. \quad (15c)$$

This is advection Eq. (2) modified due to approximation procedure. Tensor \mathbf{D}^n describes numerical diffusion, and \mathbf{T}^n - numerical dispersion. Their form depends on the accuracy of the applied approximation. If the approximation, carried out in respect of space and time, was of the second-order, then in (14) the term responsible for numerical diffusion would not appear. In case of the third-order approximation the term responsible for numerical dispersion would not appear either. The analysis of additional terms occurring in the modified equation affords information on the method's properties.

The modified advection equation (14) is similar to the advection-diffusion equation (1). In both a diffusive term exists. In the case of equation (2) this term describes the process of physical transport defined by the physical diffusion tensor \mathbf{K}^d . However, in Eq. (14) the diffusive term represents a numerical error effect resulting from the approximation of a differential equation. In analogy to Eq. (1) the tensor \mathbf{D}^n occurring in this term is called the numerical diffusivity tensor.

It is possible to determine further properties of the applied approximation executing a transformation of the co-ordinate system $x - y$ rotating it by an angle ϕ , such that the axis l is parallel and axis n normal to the velocity vector $\mathbf{w} = ui + vj$. This vector characterizes flow on the $x - y$ plain.

During rotation of the system any tensor \mathbf{R} is transformed into the new system according to the rule (Sawicki 1994):

$$\bar{\mathbf{R}} = \mathbf{Q}\mathbf{R}\mathbf{Q}^T, \quad (16)$$

where:

$$\begin{array}{ll} \bar{\mathbf{R}} & - \text{tensor in } l - n \text{ system,} \\ \mathbf{R} & - \text{tensor in } x - y \text{ system,} \\ T & - \text{transposition symbol,} \\ \mathbf{Q} = \begin{vmatrix} \cos \phi & \sin \phi \\ -\sin \phi & \cos \phi \end{vmatrix} & - \text{transformation matrix.} \end{array}$$

After multiplication (16) one obtains the tensor $\bar{\mathbf{R}}$ of the following elements:

$$\bar{R}_{11} = R_{11} \cos^2 \phi + R_{22} \sin^2 \phi + R_{12} \sin 2\phi \quad (17a)$$

$$\bar{R}_{22} = R_{11} \sin^2 \phi + R_{22} \cos^2 \phi - R_{12} \sin 2\phi \quad (17b)$$

$$\bar{R}_{12} = \bar{R}_{21} = -\frac{1}{2}(R_{11} - R_{22}) \sin 2\phi + R_{12} \cos 2\phi. \quad (17c)$$

If $\Delta x = \Delta y = \Delta$ is assumed, according to the foregoing equations, the numerical diffusivity tensor \mathbf{D}^n (15a), will have the following elements in the $l - n$ co-ordinate system (Bielecka-Kieloch 1998):

$$\begin{aligned} \bar{D}_{11}^n &= \left[\left(\theta - \frac{1}{2} \right) \Delta t u^2 + \frac{u \Delta x}{2} \right] \cos^2 \phi + \\ &+ \left[\left(\theta - \frac{1}{2} \right) \Delta t v^2 + \frac{v \Delta y}{2} \right] \sin^2 \phi + \left(\theta - \frac{1}{2} \right) \Delta t u v \sin 2\phi = \\ &= \left(\theta - \frac{1}{2} \right) \Delta t \left[(u \cos \phi + v \sin \phi)^2 \right] + \frac{\Delta}{2} (u \cos^2 \phi + v \sin^2 \phi) = \\ &= \left(\theta - \frac{1}{2} \right) \Delta t w^2 + \frac{\Delta}{2} w (\cos^3 \phi + \sin^3 \phi), \end{aligned} \quad (18a)$$

$$\begin{aligned} \bar{D}_{22}^n &= \left[\left(\theta - \frac{1}{2} \right) \Delta t u^2 + \frac{u \Delta x}{2} \right] \sin^2 \phi + \\ &+ \left[\left(\theta - \frac{1}{2} \right) \Delta t v^2 + \frac{v \Delta y}{2} \right] \cos^2 \phi - \left(\theta - \frac{1}{2} \right) \Delta t u v \sin 2\phi = \\ &= \left(\theta - \frac{1}{2} \right) \Delta t \left[(u \sin \phi - v \cos \phi)^2 \right] + \frac{\Delta}{2} (u \sin^2 \phi + v \cos^2 \phi) = \\ &= \frac{\Delta}{4} w \sin 2\phi (\sin \phi + \cos \phi), \end{aligned} \quad (18b)$$

$$\begin{aligned} \bar{D}_{12}^n &= \bar{D}_{21}^n = \\ &= -\frac{1}{2} \left\{ \left[\left(\theta - \frac{1}{2} \right) \Delta t u^2 + \frac{u \Delta x}{2} \right] - \left[\left(\theta - \frac{1}{2} \right) \Delta t v^2 + \frac{v \Delta y}{2} \right] \right\} \sin 2\phi + \\ &\quad + \left(\theta - \frac{1}{2} \right) \Delta t u v \cos 2\phi = \\ &= -\frac{1}{2} \left[\left(\theta - \frac{1}{2} \right) \Delta t (u^2 - v^2) \sin 2\phi + \left(\frac{u \Delta x}{2} - \frac{v \Delta y}{2} \right) \sin 2\phi \right] + \\ &\quad + \left(\theta - \frac{1}{2} \right) \Delta t u v (\cos^2 \phi - \sin^2 \phi) = \frac{\Delta}{4} w \sin 2\phi (\sin \phi - \cos \phi), \end{aligned} \quad (18c)$$

where $w = |\mathbf{w}|$ is a modulus of the velocity vector.

The above relations prove that the upwind scheme generates the maximum numerical diffusion, when flow is directed at an angle of 45° to an axis of the $x - y$ system, i.e. when $u = v$. For $\phi = \pi/4$ the tensor takes the following form:

$$\bar{D}^n = \begin{bmatrix} \left(\theta - \frac{1}{2}\right) \Delta t w^2 + \frac{\Delta}{2\sqrt{2}} w & 0 \\ 0 & \frac{\Delta}{2\sqrt{2}} w \end{bmatrix}. \quad (19)$$

As can be noticed, the scheme always generates some numerical diffusion in the direction normal to the velocity vector since $\bar{D}_{22}^n \neq 0$. However, the numerical diffusion in the flow direction depends on the value of the weighting parameter θ . Let us consider possible cases.

For $\theta > 1/2$ diffusion in the longitudinal direction is always greater than that in the normal direction since $\bar{D}_{11}^n > \bar{D}_{22}^n$. As a result, the initial symmetrical concentration distribution is deformed during its propagation. After a while the isolines of the distribution form ellipses of the longer axis directed longwise with the flow.

$\theta = 1/2$ means that for integration in time the second-order accuracy scheme with centered difference is adopted. The numerical diffusion in both directions is identical. Now, it is the result of the spatial derivatives approximation with first-order accuracy. The initial symmetrical concentration distribution becomes deformed after a while, however, it is still symmetrical with respect to both axes.

However, $\theta < 1/2$ influences the diffusion in the longitudinal direction, so that it is smaller than that in the normal direction, as now $\bar{D}_{11}^n < \bar{D}_{22}^n$. In the extreme case of $\theta = 0$, when

$$C_l = \frac{\Delta t \omega}{\sqrt{2} \Delta} = 1 \quad (20)$$

where C_l is the Courant number in the flow direction, the longitudinal diffusion does not occur. There is only the normal diffusion left. In the case of a flow parallel to one of the axes of the co-ordinate system, for $\theta = 0$ and the Courant number equal to one, an accurate solution is obtained. The numerical diffusion and dispersion tensors (15a, b) have zero elements. The numerical solution is in agreement with the analytical one, since the scheme is an accurate approximation of the advection equation.

Since in practical applications Courant numbers are different from one, the scheme always generates some numerical diffusion. The analysis of the dispersion tensor (15b) in this case does not bring us to any interesting conclusions. In the truncation error the terms with the second-order derivative dominate which indicates that in the solution the dissipation error plays the decisive role. The scheme produces smooth results, without oscillations, but strongly deformed by the numerical diffusion.

4. Numerical Tests

The scheme properties presented are confirmed by results of numerical tests illustrated by figures 2, 3, 4 and 5. A steady flow with a homogeneous velocity field is assumed in a reservoir of dimensions 45 m \times 45 m divided into a grid of dimensions $\Delta x = \Delta y = 1$ m. The initial condition $f(t = 0, x, y)$ is described by the Gaussian distribution of parameters $\sigma = 2$ m, $x_s = y_s = 9$ m and maximum value $f_{\max} = 1$. Assumption of $\theta = 0$ and $C_x = 1$ ($\Delta t = 10$ s) for a one-directional flow, when $u = 0.1$ m/s and $v = 0$, assures propagation of the initial distribution without deformation (Fig. 2).

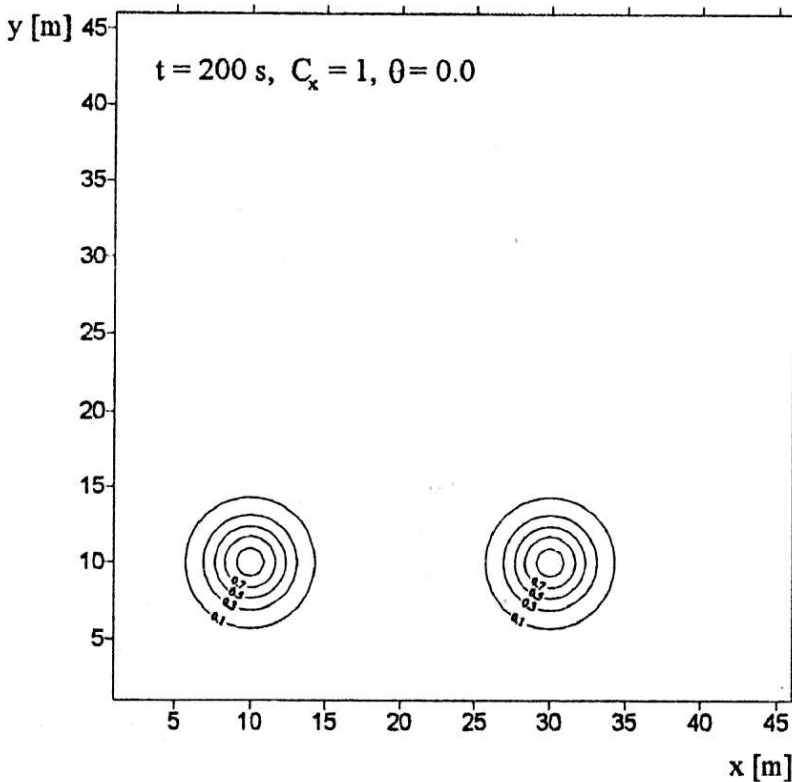


Fig. 2. Advection of the initial distribution of concentration along x axis, computed with the upwind scheme for $\theta = 0$ and $C_x = 1$

For a flow along the basin's diagonal, when $u = v = 0.1$ m/s a strong numerical diffusion always occurs. For $\theta = 1/2$ and $C_x = C_y = 1/2$ it is the same in both the longitudinal and normal direction to the velocity vector ($\bar{D}_{11}^n = \bar{D}_{22}^n$) resulting in axially symmetrical concentration distribution for $t > 0$ (Fig. 3). The maximum concentration is reduced to the value $f_{\max} = 0.182$ after $t = 200$ s.

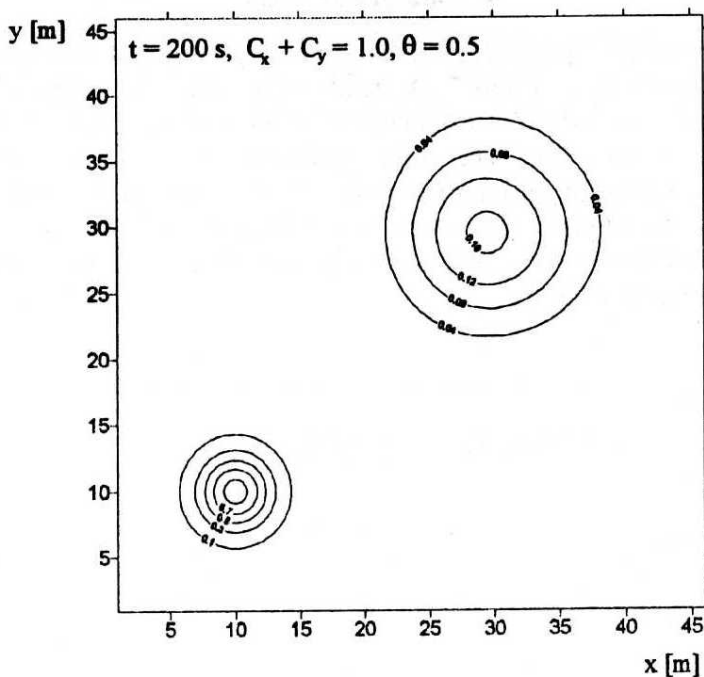


Fig. 3. Advection of the initial distribution of concentration along the diagonal, computed with the upwind scheme for $\theta = 0.5$ and $C_x + C_y = 1.0$

However, for $\theta = 1$ and $\theta = 0$ distributions axially non-symmetrical are obtained. In the first case of $\bar{D}_{11}^n > \bar{D}_{22}^n$ the distribution is stretched in the direction tangential to the velocity vector (Fig. 4). In the second case, when $\bar{D}_{11}^n < \bar{D}_{22}^n$, the distribution is stretched in the normal direction (Fig. 5). The latest result is typical for the explicit upwind scheme.

For better illustration, Fig. 6 presents concentration distributions in cross-sections situated on the reservoir's diagonal, along which advection proceeds. This allows for observation of θ parameter influence on deformation of the final solution. For instance, although the obtained distributions for $\theta = 1.0$ and $\theta = 0.0$ are stretched one in the tangential direction (Fig. 4), and the other – in normal direction (Fig. 5), the maximum concentrations are different. For $\theta = 0.0$ the maximum value of concentration (Fig. 6, curve c) is much greater than for $\theta = 1.0$ (Fig. 6, curve b). In both cases though, they are much lower than results from the accurate solution.

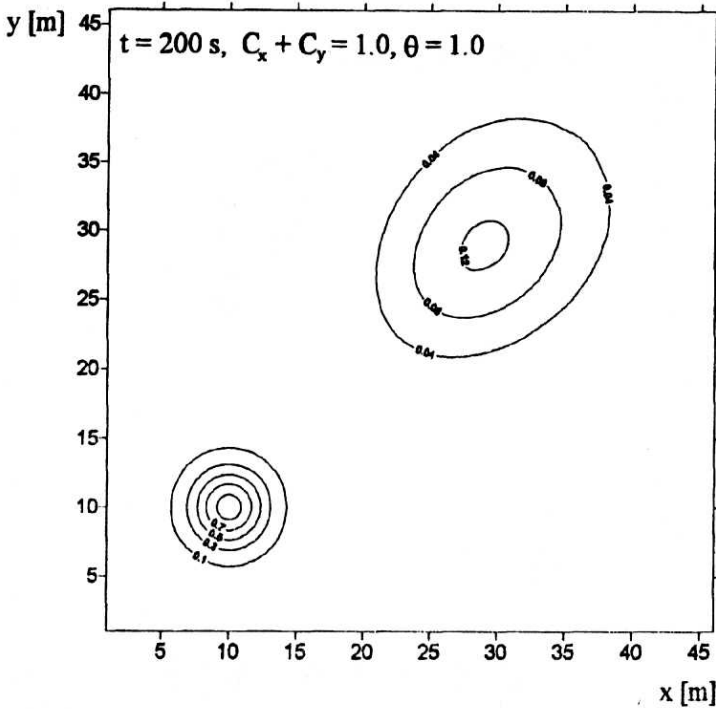


Fig. 4. Advection of the initial distribution of concentration along the diagonal, computed with the upwind scheme for $\theta = 1.0$ and $C_x + C_y = 1.0$

5. Comparison of Physical Diffusion with Numerical Diffusion

The derived tensors give another, very useful possibility – they enable comparison of physical diffusion with the numerical one. In this way it is possible to avoid excessive numerical diffusion as compared with the physical one. If the following equation

$$\frac{\partial f}{\partial t} + u_j \frac{\partial f}{\partial x_j} - \frac{\partial}{\partial x_j} \left(\mathbf{K} \frac{\partial f}{\partial x_j} \right) = 0 \quad j = 1, 2 \quad (21)$$

is solved with a dissipative scheme, i.e. generating numerical diffusion, a solution is obtained which corresponds to the following equation:

$$\frac{\partial f}{\partial t} + u_j \frac{\partial f}{\partial x_j} - \frac{\partial}{\partial x_j} \left((\mathbf{K} + \mathbf{D}^n) \frac{\partial f}{\partial x_j} \right) = 0, \quad (22)$$

- \mathbf{D}^n – numerical diffusion tensor,
- \mathbf{K} – physical diffusion tensor,
- $\mathbf{K} + \mathbf{D}^n$ – substitute tensor.

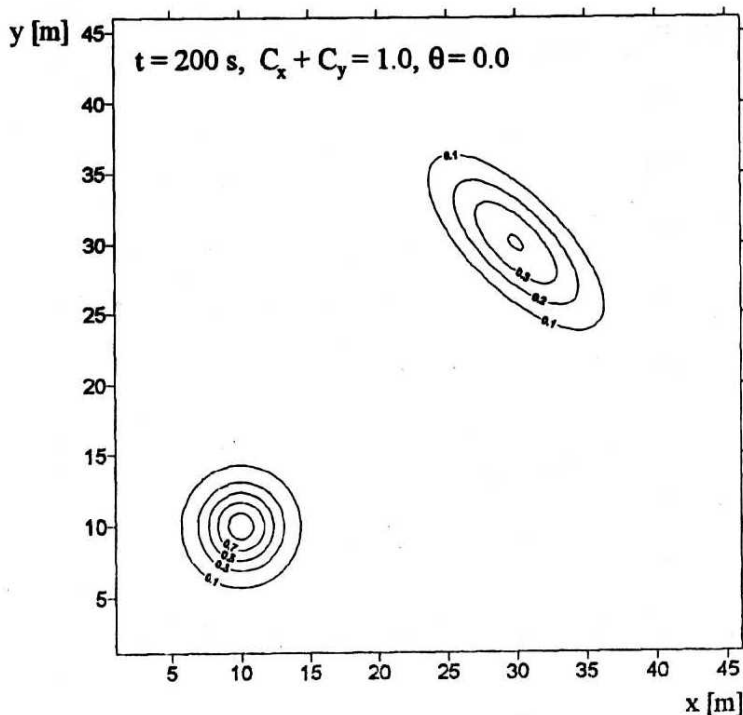


Fig. 5. Advection of the initial distribution of concentration along the diagonal, computed with the upwind scheme for $\theta = 0$ and $C_x + C_y = 1.0$

This means that in the solution, total influence of physical and numerical diffusion occurs. As a result, if numerical diffusion dominates over the physical one, an unrealistic solution is obtained. To avoid this problem it is necessary to establish a proper relation between numerical and physical diffusion. This can be achieved by a selection of appropriate grid sizes and weighting parameters. In this case it is essential to compare both tensors.

Let us present a very simple example of comparison of a physical diffusion tensor with the numerical one derived for the upwind scheme. In case of physical diffusion the most basic formula describing longitudinal (K_l) and normal (K_n) diffusion in open channels is the one proposed by Elder (Elder 1959):

$$K_l = 5.93h\nu_* \quad (23)$$

where

$$\nu_* = \sqrt{gu}/c = \sqrt{gun}/R_h^{1/6} \quad (23a)$$

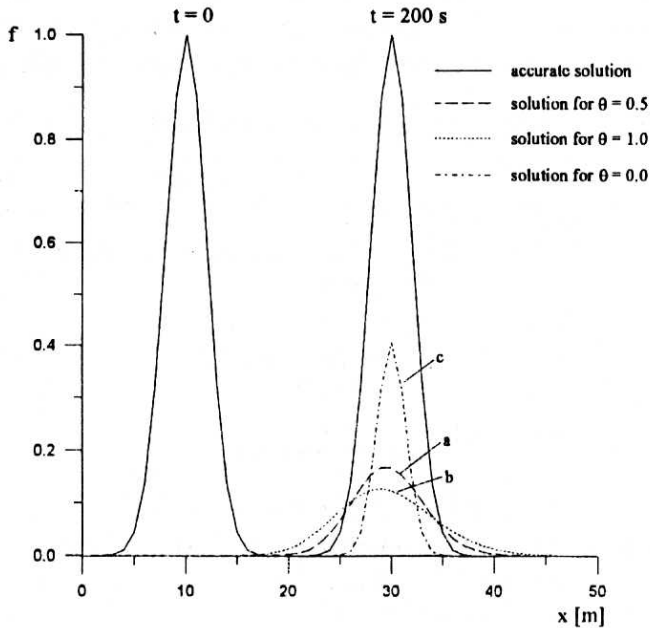


Fig. 6. Concentration distributions along the basin's diagonal, computed with the upwind scheme for $C_x + C_y = 1$ and: a) $\theta = 0.5$, b) $\theta = 1.0$, c) $\theta = 0.0$

$$c = \frac{1}{n} R_h^{1/6}$$

– Chézy coefficient (according to Manning),

$$K_n = \alpha_n h v_* = 0.23 h v_* \quad (24)$$

where $\alpha_n = 0.1 - 0.2$ for regular channels.

Using the above formulae coefficients of longitudinal (K_l) and normal (K_n) diffusion are calculated in the $l - n$ system of co-ordinates. They are compared with corresponding coefficients of numerical diffusion (\bar{D}_{ll}^n) and (\bar{D}_{nn}^n), determined for the upwind scheme. It is assumed that average flow velocity is $u = 0.1$ m/s, the Courant number is $C = 0.5$ and the following two cases, with respect to depths and grid dimensions, are considered:

1. $h = 2$ m, with which a grid of dimensions $\Delta x = \Delta y = 10$ m corresponds and
2. $h = 10$ m, with which a grid of dimensions $\Delta x = \Delta y = 100$ m corresponds.

In addition average and extreme values of Chézy and Manning coefficients are considered. The results obtained are presented in Table 1. It can be clearly noticed that in most cases longitudinal numerical diffusion dominates over the physical

as $\bar{D}_{ll}^n > K_l$. However, the normal numerical diffusion is always greater than the physical up to III orders of magnitude. Only very small grid sizes enable us to obtain comparable values of longitudinal numerical and physical diffusion.

Table 1. A comparison of physical and numerical diffusion coefficients

Depths	c	n	K_l	Grid sizes	θ	\bar{D}_{ll}^n
$h = 10$ m	24.5	0.060	0.759	$\Delta x = \Delta y = 100$ m	0	1.43
	58.7	0.025	0.314		1/2	5.00
	10	0.147	1.856		1	8.57
$h = 2$ m	18.7	0.060	0.199	$\Delta x = \Delta y = 10$ m	0	0.14
	10	0.122	0.371		1/2	0.50
$h = 10$ m	146.8	0.010	0.125		1	0.86
1468	0.001	0.013				
Depths	c	n	K_n	Grid sizes	θ	\bar{D}_{nn}^n
$h = 10$ m	24.5	0.060	0.026	$\Delta x = \Delta y = 100$ m	0	5.00
	58.7	0.025	0.010		1/2	5.00
	10	0.147	0.072		1	5.00
$h = 2$ m	18.7	0.060	0.0067	$\Delta x = \Delta y = 10$ m	0	0.50
	10	0.112	0.014		1/2	0.50
$h = 10$ m	146.8	0.010	0.0042		1	0.50
1468	0.001	0.0004				

6. Conclusions

The introduced tensors of numerical diffusion and dispersion enable clear presentation of modified by a numerical scheme 2-D advection-diffusion equation. Their analysis simplifies interpretation of numerical schemes used for solution and gives information on dissipation and dispersion errors generated by the schemes. The numerical diffusion and dispersion tensors enable easy estimation of the role of weighting parameters and their influence on the schemes properties, and in consequence – to predict a qualitative form of solution of the advection-diffusion equation.

Knowledge of the numerical diffusion tensor has two practical aspects. First it enables elimination of numerical diffusion influence by introducing a substitute tensor. Secondly, by separating the numerical diffusion effect from the solution, it enables accurate estimation of the physical diffusion tensor's components during validation of a model.

Knowledge of the numerical diffusion tensor also enables comparison of numerical diffusion coefficients with the physical diffusion coefficients and thus practical evaluation of the scheme's applicability. In case of the upwind scheme it can be stated that in most cases it generates longitudinal numerical diffusion which

is greater than the physical one. Normal numerical diffusion, however, is always greater than the physical one by one to three orders of magnitude. Only application of a very fine grid affords comparable values of numerical and physical diffusion coefficients. This scheme produces accurate results only in the case of one-dimensional flow when the Courant number is equal to one.

The fact that maximum numerical diffusion is generated when the flow is directed at an angle of 45° to the axis of a co-ordinate system, affords a practical conclusion: in order to keep the numerical diffusion lowest it is necessary to choose such a system of co-ordinates that the flow is parallel to one of the axes of the system.

In the next paper, modifications of some numerical methods, resulting from the form of numerical diffusion and dispersion tensors, will be discussed.

Acknowledgment

This paper is based on the authors Ph.D. thesis entitled: "Numerical properties of schemes applied to simulation of transport processes in open waters". The author wishes to thank Prof. Romuald Szymkiewicz for his support and supervision of the thesis.

References

- Bielecka-Kieloch M. (1998), *Numerical properties of schemes applied to simulation of transport processes in open waters*, Ph.D. thesis (in Polish), IBW PAN, Gdańsk.
- Elder J. W. (1959), The dispersion of marked fluid in turbulent shear flow, *J. Fluid Mech.*, 5, No. 4, 544-560.
- Fletcher C. A. J. (1991), *Computational techniques for fluid dynamics*, 1, Springer-Verlag, New York.
- Noye B. J. and Tan H. H. (1989), Finite difference methods for solving the two-dimensional advection-diffusion equation, *International Journal for Numerical Methods in Fluids*, 9, 75-98.
- Sawicki A. (1994), *Continuum Mechanics, Introduction* (in Polish), IBW PAN Editorial, Gdańsk.